Drosophila pVALIUM10 TRiP RNAi lines cause undesired silencing of Gateway-based transgenes

Dimitrije Stankovic[1], Gábor Csordás[2], Mirka Uhlirova[1#]

[1]Institute for Genetics and Cologne Excellence Cluster on Cellular Stress Responses in Aging-Associated Diseases (CECAD), University of Cologne, Cologne, Germany

[2]Institute of Genetics, Biological Research Centre of the Eötvös Loránd Research Network, Szeged, Hungary

[#] Address correspondence to Mirka Uhlirova, mirka.uhlirova@uni-koeln.de

Running title: pVALIUM10 TRiP lines silence Gateway-based transgenes

Keywords: *Drosophila*, RNAi, dsRNA, pValium10, Gateway recombination, TRiP lines

SUMMARY

Post-transcriptional gene silencing using double-stranded RNA has revolutionized the field of functional genetics, allowing fast and easy disruption of gene function in various organisms. In *Drosophila*, many transgenic RNAi lines have been generated in large-scale efforts, including the *Drosophila* Transgenic RNAi Project (TRiP), to facilitate *in vivo* knockdown of virtually any *Drosophila* gene with spatial and temporal resolution. The available transgenic RNAi lines represent a fundamental resource for the fly community, providing an unprecedented opportunity to address a vast range of biological questions relevant to basic and biomedical research fields. However, caution should be applied regarding the efficiency and specificity of the RNAi approach. Here, we demonstrate that pVALIUM10-based RNAi lines, representing ~11% of the total TRiP collection, cause unintended silencing of transgenes expressed from Gateway destination vectors generated via site-specific recombination. The silencing is mediated by targeting attB1 and attB2 sequences generated in the recombination reaction and included in the transcribed mRNA. Deleting these attB sites from the Gateway expression vector prevents silencing and restores expected transgene expression.

INTRODUCTION

Double-stranded RNA (dsRNA)-mediated post-transcriptional gene silencing, also known as RNA interference (RNAi), represents an ancient anti-viral defense mechanism that has been harnessed as a powerful tool for reverse functional genetics in various cultured cells, plant and animal model systems (Kennerdell & Carthew, 1998; Lohmann *et al*, 1999; Wargelius *et al*, 1999; Wianny & Zernicka-Goetz, 2000; Zamore *et al*, 2000). The dsRNA silencing relies on a highly conserved RNase III enzyme called Dicer that recognizes and processes dsRNA into small 21-23-bp segments (siRNA). Upon loading into a multiprotein RNA-induced silencing complex (RISC), the guide strand facilitates pairing with complementary on-target

41 RNAs, which are subsequently degraded by the action of the Argonaut proteins (Tomari & Zamore, 2005).
42 In *Drosophila*, spatio-temporally controlled RNAi knockdown can be achieved by expressing dsRNA using
43 transgenic binary expression systems, such as Gal4/UAS (Brand & Perrimon, 1993). The initial transgenic
44 RNAi lines were generated using plasmids with ligated inverted repeats transcribed from one (Kennerdell
45 & Carthew, 1998) or two opposite promoters (Giordano *et al*, 2002). However, these vectors were
46 unstable and not well tolerated by the bacterial strains commonly used for cloning (Hagan & Warren,
47 1983; Piccin *et al*, 2001), a problem later solved by the introduction of an intron spacer between the
48 repeats (Bao & Cagan, 2006; Lee & Carthew, 2003). This step-by-step progress led to the development of
49 the pVALIUM (Vermilion-attB-LoxP-Intron-UAS-MCS), a universal vector system for transgenic RNAi library
50 generation. The pVALIUM RNAi vectors contain an eye-color selection marker (*vermillion*), an attB site
51 enabling phiC31-mediated site-directed integration into predefined genomic locations, *white* or *ftz*
52 introns promoting the processing of dsRNA, and a cassette of two UAS pentamers, one of which is flanked
53 by loxP sites to allow tuning of the dsRNA expression levels, as well as a multiple cloning site (MCS) (Ni *et*
54 *al*, 2008).
55 The highly efficient pVALIUM10-based transgenic RNAi stocks produced within the *Drosophila* Transgenic
56 RNAi Project (TRiP) at Harvard Medical School (HMS) (https://fgr.hms.harvard.edu) represent an
57 invaluable resource for the *Drosophila* community (Perkins *et al*, 2015). At the moment of writing, 1800
58 transgenic TRiP RNAi stocks based on the pVALIUM10 are available at the Bloomington *Drosophila* stock
59 center (BDSC, https://bdsc.indiana.edu/index.html) (Perrimon *et al*, 2010). The pVALIUM10 vector carries
60 *gypsy* insulators that markedly enhance knockdown efficiency, along with two inverted "attR1-selection-
61 attR2" cassettes that facilitate cloning of dsRNA fragments via site-specific Gateway *in vitro*
62 recombineering (Ni *et al*, 2009; Reece-Hoyes & Walhout, 2018). A desired single fragment, 400 - 600 bp
63 in length and flanked by attL1 and attL2 recombination sites, can be easily moved from an entry vector

64 into a pVALIUM10 destination vector via recombination between attL and attR sites catalyzed by LR
65 clonase, producing a vector for UAS-driven expression of dsRNA (Ni *et al.*, 2009).
66 The Gateway cloning technology is also routinely used to generate transgenic constructs for expression of
67 epitope-tagged or untagged proteins, taking advantage of the *Drosophila* Gateway™ plasmid collection at
68 the *Drosophila* Genomics Resource Center (https://dgrc.bio.indiana.edu/). Importantly, as with
69 pVALIUM10 dsRNA plasmids, production of Gateway expression vectors relies on the recombination
70 between attL and attR sites resulting in the formation of attB1 and attB2 sites.
71 Here, we demonstrate that the pVALIUM10-derived RNAi lines cause undesirable knockdown of
72 transgenic reporters and overexpression lines generated with the help of the Gateway cloning technology.
73 They do so by targeting the attB sites that are part of the transcribed mRNA. Deletion of the attB1 and
74 attB2 sequences from the Gateway expression destination vector abrogates this effect and restores
75 expected transgene expression levels.
76
77
78 **RESULTS**
79 **Unexpected, non-specific silencing of the RNAse H1::GFP reporter by multiple pVALIUM10-RNAi lines**
80 *In vivo* RNAi-based genetic screens have proved very successful in identifying novel genes involved in
81 developmental and pathologic processes in a variety of *Drosophila* somatic tissues when expressed using
82 tissue-specific Gal4 driver lines (Graca *et al*, 2021; Lesch *et al*, 2010; Neely *et al*, 2010; Pletcher *et al*, 2019;
83 Port *et al*, 2011; Rotelli *et al*, 2019; Saj *et al*, 2010; Zeng *et al*, 2015; Zhou *et al*, 2019). Hence, we embarked
84 on a candidate genetic screen aimed at identifying factors controlling genome stability. During the pre-
85 screening of potential candidates we observed that expression of pVALIUM10-based *BuGZ*$^{RNAi[TRiP.JF02830]}$
86 RNAi line in the pouch region of the developing third instar wing discs, using the *nubbin-Gal4, UAS-mRFP*
87 (*nub>mRFP*) driver line, efficiently suppressed the multi-epitope tagged BuGZ transgene (*BuGZ*$^{FlyFos[v318366]}$)

88 (Sarov *et al*, 2006) (Figure 1A, B, D). A similar reduction was observed using an independent
89 *BuGZ*$^{RNAi[KK104498]}$ line from the Vienna *Drosophila* Resource Center (VDRC) KK RNAi library (Figure 1C, D).
90 Encouraged by these results, both BuGZ RNAi lines were included in the candidate genetic screen that was
91 based on expression of selected dsRNAs with the *nub>mRFP* driver. As readout for genome stability, we
92 used the ubiquitously driven RNase H1::GFP that was generated by recombining the *RNase H1* coding
93 sequence into the pUWG vector from the *Drosophila* Gateway™ plasmid collection. This resulted in the
94 expression of a C-terminally GFP-tagged RNase H1 under the control of the poly-ubiquitin promoter
95 (Figure 2A, B). The RNase H1 enzyme recognizes and resolves R-loops, DNA:RNA hybrids, that emerge
96 during transcription and represent a threat to genome stability when unresolved (Crossley *et al*, 2019;
97 Santos-Pereira & Aguilera, 2015). Unexpectedly, we observed reduction of RNase H1::GFP signal when
98 expressing *BuGZ*$^{RNAi[TRiP.JF02830]}$ but not *BuGZ*$^{RNAi[KK104498]}$ line (Figure 2C, D). Strikingly, similar downregulation
99 of RNase H1::GFP was caused by pVALIUM10-based *myc*$^{RNAi[TRiP.JF01761]}$ but not *myc*$^{RNAi[TRiP.HMS01538]}$ or
100 *myc*$^{RNAi[GD2948]}$ derived from pVALIUM20 and pMF3 vectors, respectively (Figures 1D and 2E-G). All three
101 myc-RNAi lines have been shown effective by others (Aughey *et al*, 2016; Kim-Yip & Nystul, 2018; Ledru
102 *et al*, 2022; Rust *et al*, 2018). These results indicated that the tested pVALIUM10 TRiP RNAi lines but not
103 pVALIUM20, KK or GD lines may cause "non-specific" silencing of the RNAse H1::GFP transgene. We
104 further speculated that dsRNA expressed from pVALIUM10 contains segments unrelated to the target
105 gene-specific sequences that trigger this unexpected "off-target" effect.
106
107 **pVALIUM10 RNAi and Gateway expression plasmids share attB recombination sites**
108 To identify the potential target for dsRNA-mediated knockdown of the RNAse H1::GFP transgene by
109 pVALIUM10 TRiP RNAi, we compared the plasmid sequences. We found that attB1 and attB2 sites are
110 shared between the Gateway-based expression vectors, including pUWG, and pVALIUM10 TRiP RNAi
111 plasmids. AttB1 and attB2 sites are 25 bp in length and generated by LR clonase-mediated recombination

112 between attL and attR sequences. Given the repetition of attB1 and attB2 sites, flanking the passenger
113 and guide target sequence fragments in pVALIUM10 TRiP RNAis, these sequences are transcribed and
114 could contribute to the dsRNA stem-loop substrate for Dicer. Based on these results we hypothesized that
115 dsRNAs generated from attB1 and attB2 could target, and thus silence, Gateway-based transgenes via
116 attB sites (Figure 2H).
117

118 **pVALIUM10 RNAi lines silence Gateway transgenes via attB sites**

119 To test our hypothesis, we cloned the *mCherry* coding sequence into the pUWG Gateway expression
120 vector (pUWG-*mCherry*) allowing ubiquitous expression of mCherry transcript flanked by the attB1 and
121 attB2 sites. The pUWG-*mCherry* vector then served as a template for overlap PCR to generate the
122 pUWG$^{\Delta attB}$-*mCherry* construct that lacks attB sites (Figure 3A). Both plasmids were used to establish
123 transgenic fly lines through a standard *Drosophila* germline transformation method (Rubin & Spradling,
124 1982). The susceptibility or resistance of *ubi-mCherry* (pUWG-*mCherry*) and *ubi$^{\Delta attB}$-mCherry* (pUWG$^{\Delta attB}$-
125 *mCherry*) transcripts to RNAi-mediated silencing was then tested by driving various RNAi lines under the
126 control of the *nub-Gal4* driver. Immunostaining of the third instar wing imaginal discs using an anti-RFP
127 antibody revealed an identical pattern of ubi-mCherry and ubi$^{\Delta attB}$-mCherry transgenes in the control
128 (*nub>*) background (Figure 3B, C). In contrast, levels of ubi-mCherry but not ubi$^{\Delta attB}$-mCherry transgenic
129 protein were markedly reduced in the wing pouch region relative to the rest of the tissue following
130 overexpression of *BuGZ* and *myc* pVALIUM10 TRiP RNAi lines (Figure 3D, E, H, I, L, M) while no significant
131 changes were observed when *BuGZ* and *myc* were knockdown using KK and pVALIUM20 RNAi lines,
132 respectively (Figure 3F, G, J, K, L, M). Importantly, the attB site-dependent silencing of ubi-mCherry was
133 recapitulated using additional set of pVALIUM10 TRiP RNAi lines targeting *Atf3*, *Lip4*, *yki*, *DH44*, *ftz-f1*,
134 *mago*, *brat*, and *Actβ* genes (Supplementary Figure S1).

135 Finally, we tested whether pVALIUM10 TRiP RNAi lines may also interfere with UAS-inducible attB-
136 containing transcripts, such as transgenic fly open reading frames (ORFs) expressed from the Gateway
137 destination vector pGW-HA.attB (Bischof *et al*, 2014). To this end, we assessed levels of the HA-tagged
138 SmD3 FlyORF protein in the presence of pVALIUM10 or KK BuGZ-RNAi line. In contrast to a strong
139 enrichment of SmD3::3xHA protein in the wing pouch cells of control (*nub>*) and *BuGZ*$^{RNAi[KK104498]}$
140 expressing wing discs, the signal was noticeably reduced in *nub>BuGZ*$^{RNAi[TRiP.JF02830]}$ cells (Figure 3N-P).
141 These results strongly indicate that the dsRNA hairpin produced from pVALIUM10 RNAi vectors generates
142 attB1- and attB2-siRNAs, which guide destruction of transcripts containing such target sites. This off-target
143 silencing via attB sites is specific to RNAi lines based on pVALIUM10. Absence of attB1 and attB2 sites
144 renders the Gateway-derived transcript resistant to pVALIUM10 TRiP RNAi.
145
146
147 **DISCUSSION**
148 The use of transgenic RNAi to achieve developmental stage- and tissue-specific knockdown of candidate
149 genes and to perform genome-wide screens in *Drosophila* has become commonplace in the past two
150 decades (Blake *et al*, 2017; Dietzl *et al*, 2007; Hu *et al*, 2017; Port *et al.*, 2011). Both, our knowledge on
151 the RNAi mechanism, and the tools to generate new types of RNAi constructs efficiently have considerably
152 evolved in recent years. As a result, several independent transgenic RNAi stock collections were
153 established, including Vienna *Drosophila* stock center (VDRC, 12,671 RNAi lines,
154 https://stockcenter.vdrc.at/control/main), Bloomington *Drosophila* Stock Center (BDSC, 13,698 RNAi
155 lines, https://bdsc.indiana.edu/), and the National Institute of Genetics (NIG, 12,368 RNAi lines,
156 https://shigen.nig.ac.jp/fly/nigfly/) at the time of writing. Yet, in spite of being a broadly used technique,
157 transgenic manipulation of gene expression can still have unforeseen consequences. Recently, a large
158 portion of the RNAi lines from the VDRC KK collection were found to produce phenotypes due to a

159 secondary insertion and consequent ectopic expression of the *tiptop* gene (Green *et al*, 2014; Vissers *et*
160 *al*, 2016). More recently, van der Graaf and colleagues reported that transgenes inserted in the commonly
161 used *attP40* landing site on the second chromosome can decrease the expression of Msp300, a member
162 of the LINC complex, and hence lead to nuclear size, shape and positioning phenotypes (van der Graaf *et*
163 *al*, 2022).
164 Here, we demonstrate that the pVALIUM10-based RNAi lines cause unintended silencing of ORFs
165 expressed from Gateway expression vectors or potentially any transcripts containing attB1 and attB2
166 sites. We show that the removal of these sites abrogates the undesirable knockdown. Given the popularity
167 of the Gateway expression vectors to generate transgenic protein-reporters and tagged overexpression
168 constructs, our results suggest that simultaneous use of pVALIUM10 TRiP RNAi may lead to experimental
169 artefacts unrelated to the investigated biological process.
170 Of note, in the original publication of pVALIUM10 vectors, the authors tested for potential off-target
171 effects by comparing the hairpin sequence against the *Drosophila* genome (Ni *et al.*, 2009), which does
172 not contain endogenous 21nt stretches equivalent to the attB1 and attB2 sequences. However, as the
173 transgenic toolkit in *Drosophila* is ever expanding, each additional transgene has the possibility to produce
174 a synthetic effect with the existing RNAi lines. Hence, we suggest that the researchers validate the type
175 of TRiP RNAi line or the expression vector sequence before commencing their experiments. As an
176 example, we do not recommend combining RNAi based on pVALIUM10 with the 3xHA-tagged
177 overexpression lines from FlyORF (https://flyorf.ch), as the latter was also generated via Gateway reaction
178 and contains attB sites flanking the inserted ORF (Bischof *et al.*, 2014), which can lead to undesired
179 silencing of the transcript. Furthermore, this finding reinforces the idea that RNAi experiments should
180 adhere to the standards established in the past decades, including investigating possible off-target effects
181 to eliminate knockdown of the unintended gene, using multiple independent RNAi lines to recapitulate

182 phenotypes, and confirming the knockdown of the targeted gene products (Echeverri *et al*, 2006; Green
183 *et al.*, 2014; Kaya-Çopur & Schnorrer, 2016).
184
185
186 **MATERIALS AND METHODS**
187 **Fly stocks and Husbandry**
188 The following *Drosophila* strains were used: w^{1118} (BDSC; RRID: BDSC_3605), *nubbin-Gal4, UAS-myr-mRFP*
189 (*nub>mRFP*), $BuGZ^{FlyFos[v318366]}$ (VDRC), $BuGZ^{RNAi[TRiP.JF02830]}$ (BDSC; RRID:BDSC_27996), $BuGZ^{RNAi[KK104498]}$
190 (VDRC), $Lip4^{RNAi[TRiP.HMO5136]}$ (BDSC; RRID:BDSC_28925), $myc^{RNAi[TRiP.JF01761]}$ (BDSC; RRID:BDSC_25783),
191 $myc^{RNAi[TRiP.HMS01538]}$ (BDSC; RRID:BDSC_36123), $myc^{RNAi[GD2948]}$ (VDRC), $Act\beta^{RNAi[TRiP.JF03276]}$ (BDSC;
192 RRID:BDSC_29597), $ftz\text{-}f1^{RNAi[TRiP.JF02738]}$ (BDSC; RRID:BDSC_27659), $yki^{RNAi[TRiP.JF03119]}$ (BDSC;
193 RRID:BDSC_31965), $Atf3^{RNAi[TRiP.JF02303]}$ (BDSC; RRID:BDSC_26741), $DH44^{RNAi[TRiP.JF01822]}$ (BDSC;
194 RRID:BDSC_25804), $brat^{RNAi[TRiP.HM05078]}$ (BDSC; RRID:BDSC_28590), $mago^{RNAi[TRiP.HM05142]}$ (BDSC;
195 RRID:BDSC_28931), $SmD3::3xHA^{[FlyORF\ F003987]}$ (FlyORF), $nub>SmD3::3xHA^{[FlyORF\ F003987]}$ (Erkelenz *et al*, 2021),
196 *ubi-RNase H1::GFP*, *ubi-mCherry*, $ubi^{\Delta attB}$*-mCherry* (this study). All *Drosophila* stocks are listed in
197 Supplementary Table S1. All crosses were set up and maintained at 25 °C, unless specified otherwise, on
198 a diet consisting of 0.8% agar, 8% cornmeal, 1% soymeal, 1.8% dry yeast, 8% malt extract, and 2.2% sugar-
199 beet syrup, which was supplemented with 0.625% propionic acid and 0.15% Nipagin. w^{1118} line was used
200 as control.
201
202 **Generation of plasmids and transgenic lines**
203 The open reading frame of *rnh1* (FBgn0023171) was amplified from *Drosophila melanogaster* cDNA (w^{1118})
204 using primers harboring NotI and SalI restriction sites. The stop codon was excluded to allow C-terminal
205 tagging of the protein. The ORF was cloned into the Gateway pENTR4 Dual Selection Vector (Thermo

206 Fisher Scientific; #A10465). The ORF was then recombined into the pUWG vector (DGRC; #1284) using the
207 LR Clonase II enzyme mix according to manufacturer's instructions (Thermo Fisher Scientific; #11791020).
208 The coding sequence of *mCherry* (GenBank: AY678264.1) was amplified with specific primers, cloned into
209 the pENTR 4 Dual Selection vector (Invitrogen, Cat. Nr. #A10465) including a stop codon and subsequently
210 recombined into the pUWG vector (pUWG-*mCherry*). Overlap PCR strategy was employed to generate the
211 pUWG$^{\Delta attB}$-*mCherry* construct lacking attB sites resulting from the LR recombination. Three separate PCR
212 reactions were performed to produce fragments for assembly using the original pUWG-*mCherry* plasmid
213 as a template. The forward primer of the first primer pair contained a XhoI restriction site, while the
214 reverse primer contained a XbaI restriction site. Partial complementarity of the reverse and forward
215 primers used to synthesize the downstream fragment enabled the exclusion of attB sites in the final
216 product. The final PCR product was ligated into the pUWG-*mCherry* plasmid digested with XbaI and XhoI.
217 Transgenic fly lines with random insertions of the constructs were generated by standard P-element-
218 mediated transformation using w^{1118} *Drosophila* strain. All primers and plasmids are listed in
219 Supplementary Table S2.
220
221 **Tissue dissection and immunostaining**
222 Wing imaginal discs dissected from third instar *Drosophila* larvae (7 days after egg laying (AEL)) were fixed
223 for 25 minutes with 4% paraformaldehyde in PBS containing 0.1% Triton X (PBS-T) at room temperature.
224 Fixed tissues were washed 3 times with PBS-T. Primary antibodies were diluted in blocking buffer (PBS-T
225 with 0.3% BSA) and tissues were stained overnight at 4 °C. The following primary antibodies were used:
226 rabbit anti-mRFP (1:500, MBL International Cat# PM005, RRID:AB_591279), goat anti-GFP (1:500, Abcam
227 Cat# ab6673, RRID:AB_305643), and rabbit-anti HA (1:1000, Abcam Cat# ab9110, RRID:AB_307019). After
228 washing, the samples were incubated with the corresponding Alexa Fluor 488 (1:2000, Thermo Fisher
229 Scientific Cat# A-11034, RRID:AB_2576217), Cy2 (1:2000, Jackson ImmunoResearch Labs Cat# 705-225-

230 147, RRID:AB_2307341) or Cy3 (Jackson ImmunoResearch Labs Cat# 711-165-152, RRID:AB_2307443)
231 conjugated secondary antibodies overnight at 4 °C, washed and counterstained with DAPI (1:1000 dilution
232 of 5 mg/ml stock, 6335.1, Carl Roth GmbH) to visualize nuclei. Tissues were mounted on glass slides in
233 Dabco-Mowiol 4-88 (Sigma-Aldrich Cat# D2522 and Cat# 81381).
234
235 **Image acquisition and processing**
236 Confocal images and stacks were acquired with Olympus FV1000 confocal microscope equipped with 20X
237 UPlan S-Apo (NA 0.85), 40X UPlan FL (NA 1.30) and 60X UPlanApo (NA1.35) objectives. Maximum Z-
238 projections were generated from consecutive sections taken at 1.4 µm steps using Fluoview 1000
239 Software (Olympus) (RRID: SCR_014215) and Fiji (https://fiji.sc/) (RRID:SCR_002285). Final image
240 processing, including panel assembly, brightness and contrast adjustments were performed in Adobe
241 Photoshop CC (Adobe Systems, Inc.) (RRID:SCR_014199).
242
243 **Quantification of mCherry signal intensity**
244 Fluorescent signal intensity was quantified with Fiji (https://fiji.sc/) (RRID:SCR_002285). A square
245 selection was created in the middle of the pouch region, and the „Mean intensity" was measured, then
246 the same selection was moved to the middle of the notum and the measurement was repeated. The two
247 values were divided to produce a pouch/notum intensity ratio for each wing disc. Statistical significance
248 was determined by one-way ANOVA with Tukey's multiple comparison test in GraphPad Prism
249 (RRID:SCR_002798).
250
251

252 **ACKNOWLEDGEMENTS**

253 We thank Norbert Perrimon for discussions and comments on the manuscript. We thank the Bloomington
254 *Drosophila* Stock Center (BDSC, Bloomington, IN, USA), the Vienna *Drosophila* Resource Center (VDRC,
255 Vienna, Austria), *Drosophila* Genomic Resource Center (DGRC, supported by NIH grant 2P40OD010949,
256 Bloomington, IN, USA), the Zurich ORFeome Project (FlyORF, Zurich, Switzerland) for fly stocks and
257 plasmids. We are grateful to Tina Bresser for generation of transgenic lines and Nils Teuscher for fly stock
258 maintenance and technical assistance.

259

260

261 **REFERENCES**

262 Aughey GN, Grice SJ, Liu J-L (2016) The Interplay between Myc and CTP Synthase in Drosophila. *PLOS*
263 *Genetics* 12: e1005867

264 Bao S, Cagan R (2006) Fast cloning inverted repeats for RNA interference. *RNA* 12: 2020-2024

265 Bischof J, Sheils EM, Björklund M, Basler K (2014) Generation of a transgenic ORFeome library in
266 Drosophila. *Nature protocols* 9: 1607-1620

267 Blake AJ, Finger DS, Hardy VL, Ables ET (2017) RNAi-Based Techniques for the Analysis of Gene Function
268 in Drosophila Germline Stem Cells. *Methods in molecular biology (Clifton, NJ)* 1622: 161-184

269 Brand AH, Perrimon N (1993) Targeted gene expression as a means of altering cell fates and generating
270 dominant phenotypes. *Development* 118: 401-415

271 Crossley MP, Bocek M, Cimprich KA (2019) R-Loops as Cellular Regulators and Genomic Threats. *Mol Cell*
272 73: 398-411

273 Dietzl G, Chen D, Schnorrer F, Su KC, Barinova Y, Fellner M, Gasser B, Kinsey K, Oppel S, Scheiblauer S *et*
274 *al* (2007) A genome-wide transgenic RNAi library for conditional gene inactivation in Drosophila. *Nature*
275 448: 151-156

276 Echeverri CJ, Beachy PA, Baum B, Boutros M, Buchholz F, Chanda SK, Downward J, Ellenberg J, Fraser
277 AG, Hacohen N *et al* (2006) Minimizing the risk of reporting false positives in large-scale RNAi screens.
278 *Nature Methods* 3: 777-779

279 Erkelenz S, Stankovic D, Mundorf J, Bresser T, Claudius AK, Boehm V, Gehring NH, Uhlirova M (2021) Ecd
280 promotes U5 snRNP maturation and Prp8 stability. *Nucleic Acids Res* 49: 1688-1707

281 Giordano E, Rendina R, Peluso I, Furia M (2002) RNAi triggered by symmetrically transcribed transgenes
282 in Drosophila melanogaster. *Genetics* 160: 637-648

283 Graca FA, Sheffield N, Puppa M, Finkelstein D, Hunt LC, Demontis F (2021) A large-scale transgenic RNAi
284 screen identifies transcription factors that modulate myofiber size in Drosophila. *PLOS Genetics* 17:
285 e1009926

286 Green EW, Fedele G, Giorgini F, Kyriacou CP (2014) A Drosophila RNAi collection is subject to dominant
287 phenotypic effects. *Nat Methods* 11: 222-223

288 Hagan CE, Warren GJ (1983) Viability of palindromic DNA is restored by deletions occurring at low but
289 variable frequency in plasmids of Escherichia coli. *Gene* 24: 317-326

290 Hu Y, Comjean A, Roesel C, Vinayagam A, Flockhart I, Zirin J, Perkins L, Perrimon N, Mohr SE (2017)
291 FlyRNAi.org-the database of the Drosophila RNAi screening center and transgenic RNAi project: 2017
292 update. *Nucleic Acids Res* 45: D672-D678

293 Kaya-Çopur A, Schnorrer F (2016) A Guide to Genome-Wide In Vivo RNAi Applications in Drosophila.
294 *Methods Mol Biol* 1478: 117-143

295 Kennerdell JR, Carthew RW (1998) Use of dsRNA-mediated genetic interference to demonstrate that
296 frizzled and frizzled 2 act in the wingless pathway. *Cell* 95: 1017-1026

297 Kim-Yip RP, Nystul TG (2018) Wingless promotes EGFR signaling in follicle stem cells to maintain self-
298 renewal. *Development* 145: dev168716

299 Ledru M, Clark CA, Brown J, Verghese S, Ferrara S, Goodspeed A, Su TT (2022) Differential gene
300 expression analysis identified determinants of cell fate plasticity during radiation-induced regeneration
301 in Drosophila. *PLoS Genet* 18: e1009989

302 Lee YS, Carthew RW (2003) Making a better RNAi vector for Drosophila: use of intron spacers. *Methods*
303 30: 322-329

304 Lesch C, Jo J, Wu Y, Fish GS, Galko MJ (2010) A targeted UAS-RNAi screen in Drosophila larvae identifies
305 wound closure genes regulating distinct cellular processes. *Genetics* 186: 943-957

306 Lohmann JU, Endl I, Bosch TC (1999) Silencing of developmental genes in Hydra. *Dev Biol* 214: 211-214

307 Neely GG, Kuba K, Cammarato A, Isobe K, Amann S, Zhang L, Murata M, Elmen L, Gupta V, Arora S *et al*
308 (2010) A global in vivo Drosophila RNAi screen identifies NOT3 as a conserved regulator of heart
309 function. *Cell* 141: 142-153

310 Ni JQ, Liu LP, Binari R, Hardy R, Shim HS, Cavallaro A, Booker M, Pfeiffer BD, Markstein M, Wang H *et al*
311 (2009) A Drosophila resource of transgenic RNAi lines for neurogenetics. *Genetics* 182: 1089-1100

312 Ni JQ, Markstein M, Binari R, Pfeiffer B, Liu LP, Villalta C, Booker M, Perkins L, Perrimon N (2008) Vector
313 and parameters for targeted transgenic RNA interference in Drosophila melanogaster. *Nat Methods* 5:
314 49-51

315 Perkins LA, Holderbaum L, Tao R, Hu Y, Sopko R, McCall K, Yang-Zhou D, Flockhart I, Binari R, Shim HS *et*
316 *al* (2015) The Transgenic RNAi Project at Harvard Medical School: Resources and Validation. *Genetics*
317 201: 843-852

318 Perrimon N, Ni JQ, Perkins L (2010) In vivo RNAi: today and tomorrow. *Cold Spring Harb Perspect Biol* 2:
319 a003640

320 Piccin A, Salameh A, Benna C, Sandrelli F, Mazzotta G, Zordan M, Rosato E, Kyriacou CP, Costa R (2001)
321 Efficient and heritable functional knock-out of an adult phenotype in Drosophila using a GAL4-driven
322 hairpin RNA incorporating a heterologous spacer. *Nucleic Acids Research* 29

323 Pletcher RC, Hardman SL, Intagliata SF, Lawson RL, Page A, Tennessen JM (2019) A Genetic Screen Using
324 the Drosophila melanogaster TRiP RNAi Collection To Identify Metabolic Enzymes Required for Eye
325 Development. *G3 (Bethesda)* 9: 2061-2070

326 Port F, Hausmann G, Basler K (2011) A genome-wide RNA interference screen uncovers two p24 proteins
327 as regulators of Wingless secretion. *EMBO Rep* 12: 1144-1152

328 Reece-Hoyes JS, Walhout AJM (2018) Gateway Recombinational Cloning. *Cold Spring Harb Protoc* 2018:
329 pdb.top094912

330 Rotelli MD, Bolling AM, Killion AW, Weinberg AJ, Dixon MJ, Calvi BR (2019) An RNAi Screen for Genes
331 Required for Growth of Drosophila Wing Tissue. *G3 Genes|Genomes|Genetics* 9: 3087-3100

332 Rubin GM, Spradling AC (1982) Genetic transformation of Drosophila with transposable element vectors.
333 *Science* 218: 348-353

334 Rust K, Tiwari MD, Mishra VK, Grawe F, Wodarz A (2018) Myc and the Tip60 chromatin remodeling
335 complex control neuroblast maintenance and polarity in Drosophila. *EMBO J* 37

336 Saj A, Arziman Z, Stempfle D, van Belle W, Sauder U, Horn T, Dürrenberger M, Paro R, Boutros M,
337 Merdes G (2010) A Combined Ex Vivo and In Vivo RNAi Screen for Notch Regulators in Drosophila
338 Reveals an Extensive Notch Interaction Network. *Developmental Cell* 18: 862-876

339 Santos-Pereira JM, Aguilera A (2015) R loops: new modulators of genome dynamics and function. *Nat*
340 *Rev Genet* 16: 583-597

341 Sarov M, Schneider S, Pozniakovski A, Roguev A, Ernst S, Zhang Y, Hyman AA, Stewart AF (2006) A
342 recombineering pipeline for functional genomics applied to Caenorhabditis elegans. *Nat Methods* 3:
343 839-844

344 Tomari Y, Zamore PD (2005) Perspective: machines for RNAi. *Genes Dev* 19: 517-529

345 van der Graaf K, Srivastav S, Singh P, McNew JA, Stern M (2022) The Drosophila attP40 docking site and
346 derivatives are insertion mutations of MSP300. *bioRxiv*: 2022.2005.2014.491875

347 Vissers JH, Manning SA, Kulkarni A, Harvey KF (2016) A Drosophila RNAi library modulates Hippo
348 pathway-dependent tissue growth. *Nat Commun* 7: 10368

349 Wargelius A, Ellingsen S, Fjose A (1999) Double-stranded RNA induces specific developmental defects in
350 zebrafish embryos. *Biochem Biophys Res Commun* 263: 156-161

351 Wianny F, Zernicka-Goetz M (2000) Specific interference with gene function by double-stranded RNA in
352 early mouse development. *Nat Cell Biol* 2: 70-75

353 Zamore PD, Tuschl T, Sharp PA, Bartel DP (2000) RNAi: double-stranded RNA directs the ATP-dependent
354 cleavage of mRNA at 21 to 23 nucleotide intervals. *Cell* 101: 25-33

355 Zeng X, Han L, Singh SR, Liu H, Neumuller RA, Yan D, Hu Y, Liu Y, Liu W, Lin X *et al* (2015) Genome-wide
356 RNAi screen identifies networks involved in intestinal stem cell regulation in Drosophila. *Cell Rep* 10:
357 1226-1238

358 Zhou J, Xu L, Duan X, Liu W, Zhao X, Wang X, Shang W, Fang X, Yang H, Jia L *et al* (2019) Large-scale RNAi
359 screen identified Dhpr as a regulator of mitochondrial morphology and tissue homeostasis. *Science*
360 *Advances* 5: eaax0365
361

362

Figure 1

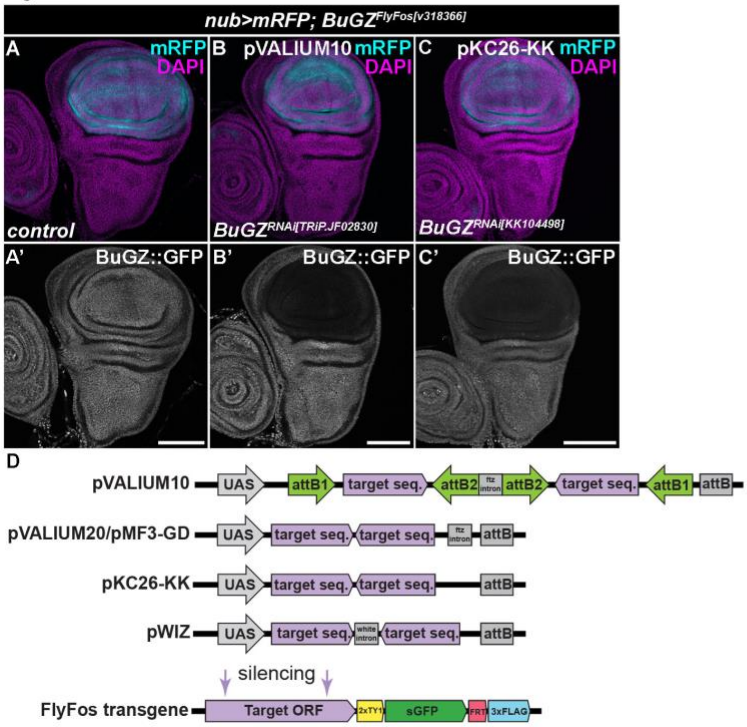

Figure 1. pVALIUM10 and KK RNAi lines cause efficient silencing.

(A-C) Expression of pVALIUM10 BuGZ$^{RNAi[TRIP.JF02830]}$ (B, B') and KK-based BuGZ$^{RNAi[KK104498]}$ transgenic RNAi lines (C, C') using the *nubbin-Gal4, UAS-myr-mRFP* driver (*nub>mRFP*, light blue) causes a marked reduction of a BuGZ$^{FlyFos[v318366]}$ transgenic protein in the pouch region of WDs relative to the hinge and notum, and control WD (A, A'). Micrographs show projections of multiple confocal sections of WDs dissected from third instar larvae 7 days AEL. The multiple-tagged BuGZ$^{FlyFos\ [v318366]}$ protein was visualized by immunostaining with an anti-GFP antibody (white). Nuclei were counterstained with DAPI (magenta). Scale bars: 100 μm. **(D)** Schematic representation of various vectors used for cloning and overexpression of dsRNA. In the absence of the target-specific antibody, the RNAi efficacy can be assessed with the help of FlyFos transgenes expressing multiple-tagged proteins under the control of the endogenous regulatory sequences.

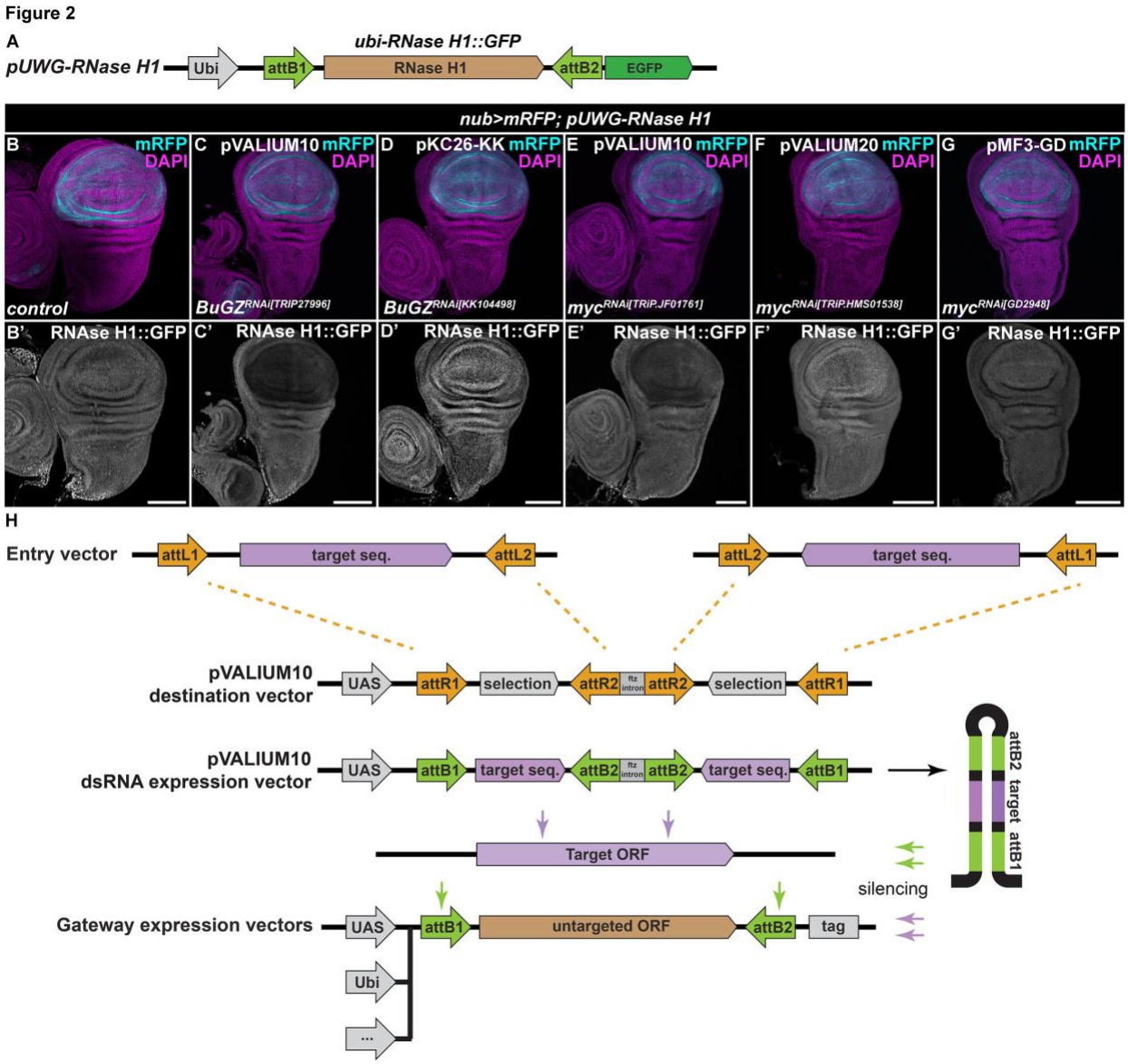

Figure 2. pVALIUM10-based lines cause non-specific silencing of the RNAse H1::GFP transgenic reporter. **(A)** Schematic representation of the transgenic *pUWG-RNase H1* reporter construct expressing the C-terminally-tagged RNase H1::GFP protein from the ubiquitous (*ubi*) promoter. The *RNase H1* coding sequence is flanked by attB1 and attB2 sites generated via Gateway-mediated recombination catalyzed by the LR clonase. **(B-G)** Immunostaining with a GFP-specific antibody revealed a marked reduction of the RNase H1::GFP levels in the nubbin domain (mRFP, light blue), where pVALIUM10-based *BuGZ*$^{RNAi[TRIP.JF02830]}$ (C) and *myc*$^{RNAi[TRiP.JF01761]}$ (E) RNAi lines were expressed using the *nubbin-Gal4, UAS-myr-*

384 *mRFP* driver (*nub>mRFP*). No such downregulation of the RNase H1::GFP signal was observed in control
385 WD (B) and following expression of KK-based *BuGZ*$^{RNAi[KK104498]}$ (D), pVALIUM20-based *myc*$^{RNAi[TRiP.HMS01538]}$
386 (F) or GD-based *myc*$^{RNAi[GD2948]}$ (G). Micrographs show projections of multiple confocal sections of WDs
387 dissected from third instar larvae 7 days AEL. Nuclei were counterstained with DAPI (magenta). Scale bars:
388 100 μm. **(H)** Generation of pVALIUM10 RNAi lines relied on a LR clonase-mediated recombination of
389 dsRNA fragment from an Entry vector to the pVALIUM10 destination vector (Ni *et al.*, 2009). The dsRNA
390 hairpin produced from the pVALIUM10 dsRNA expression vector is the source of siRNA species targeting
391 the transcript of interest (target ORF) but also attB1 and attB2 sites present in any of the Gateway
392 expression vectors generated via the same recombination mechanisms.
393

Figure 3

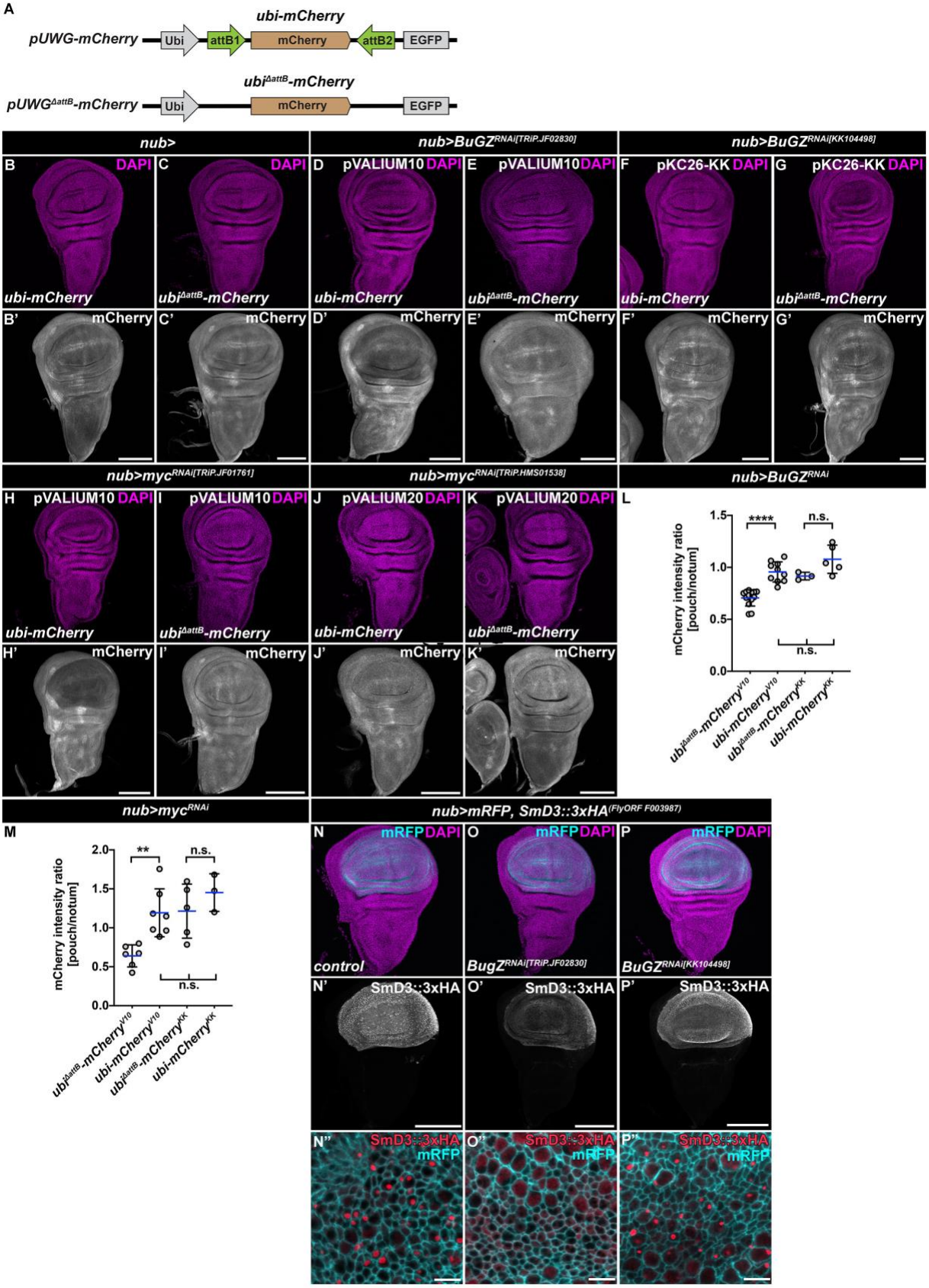
A
ubi-mCherry
pUWG-mCherry
Ubi
attB1
mCherry
attB2
EGFP
ubiΔattB-mCherry
pUWGΔattB-mCherry
nub>
nub>BuGZRNAi[TRiP.JF02830]
nub>BuGZRNAi[KK104498]
DAPI
pVALIUM10
pKC26-KK
mCherry
nub>mycRNAi[TRiP.JF01761]
nub>mycRNAi[TRiP.HMS01538]
nub>BuGZRNAi
pVALIUM20
mCherry intensity ratio [pouch/notum]
****
n.s.
nub>mycRNAi
**
nub>mRFP, SmD3::3xHA(FlyORF F003987)
mRFP
control
BugZRNAi[TRiP.JF02830]
BuGZRNAi[KK104498]
SmD3::3xHA

394

395 **Figure 3. pVALIUM10 RNAi lines silence Gateway transgenes via attB1 and attB2 sites.**

396 **(A)** Schematic of the transgenic wild-type *pUWG-mCherry* and mutant *pUWG*$^{\Delta attB}$*-mCherry* reporter
397 constructs. The mCherry is expressed from the ubiquitous (*ubi*) promoter. **(B, C)** Wild type *ubi-mCherry*
398 and mutant *ubi*$^{\Delta attB}$*-mCherry* reporters showed similar expression pattern in the wing imaginal discs. **(D-**
399 **K)** Wild-type *ubi-mCherry* was efficiently downregulated by pVALIUM10 *BuGZ*$^{RNAi[TRIP.JF02830]}$ and
400 *myc*$^{RNAi[TRiP.JF01761]}$ expressed under the control of the *nubbin-Gal4* driver (*nub>*) relative to the rest of the
401 WD (D, H). In contrast, absence of attB1 and attB2 sequences rendered the *ubi*$^{\Delta attB}$*-mCherry* reporter
402 resistant to pVALIUM10 RNAi-mediated silencing (E, I). Neither KK- (*BuGZ*$^{RNAi[KK104498]}$) nor pVALIUM20-
403 based (*myc*$^{RNAi[TRiP.HMS01538]}$) RNAi lines affected mCherry levels expressed from the wild-type or mutant
404 reporter constructs (F, G, J, K). Micrographs show projections of multiple confocal sections of WDs
405 dissected from third instar larvae 7 days AEL that were immunostained with an anti-mRFP antibody
406 (white). Nuclei were counterstained with DAPI (magenta). Scale bars: 100 μm. **(L, M)** Quantification of
407 mCherry signal depicted as relative intensity ratio between the pouch and notum region. Statistical
408 significance was determined by one-way ANOVA with Tukey's multiple comparison test; $n \geq 3$; **$p<0.01$,
409 ****$p<0.0001$, n.s. non-significant. **(N-P)** Expression of pVALIUM10 *BuGZ*$^{RNAi[TRIP.JF02830]}$ (O) in the wing
410 pouch using *nubbin-Gal4, UAS-mRFP* driver (*nub>mRFP*) reduces SmD3::3xHA levels compared to control
411 (N) and KK-BuGZ-RNAi (*BuGZ*$^{RNAi[KK104498]}$) (P). Note foci of SmD3::3xHA protein in control (N") and
412 *BuGZ*$^{RNAi[KK104498]}$ cells (P") cells that are not present in *BuGZ*$^{RNAi[TRIP.JF02830]}$ expressing cells (O"). Micrographs
413 show projections of multiple or single (N"-P") confocal sections of WDs dissected from third instar larvae
414 7 days AEL that were immunostained with an anti-HA antibody (white, N'-P'; red, N"-P"). Nuclei were
415 counterstained with DAPI (magenta). Scale bars: 100 μm or 5 μm (N"-P").